



AMERICAN JOURNAL OF MULTIDISCIPLINARY RESEARCH AND INNOVATION (AJMRI)

ISSN: 2158-8155 (ONLINE)

VOLUME 1 ISSUE 2 (2022)



PUBLISHED BY: E-PALLI, DELAWARE, USA

Template-Free Synthesis and Control Drug Release of Calcium Carbonate-Hydroxylapatite Composite

Sulemana Yahaya¹, Tarlutu Ibrahim¹ and Abdul-Rauf Ibrahim^{2*}

Article Information

Received: May 06, 2022

Accepted: May 25, 2022

Published: May 28, 2022

Keywords

CO₂-expanded carbonation, Hydroxylapatite, Composite, Drug delivery agent, Control release

ABSTRACT

We employed Gas expanded liquids (GXLs) technology to synthesize calcium carbonate-hydroxylapatite composite (CaCO₃-HAp) nanoparticles and investigated the effects of reaction parameters on the properties of the composites as well as the performance of the composites as drug delivery agent using ibuprofen as a model drug in simulated gastric fluid. Separately, calcium carbonate and hydroxylapatite have been used extensively in pharmaceutical and drug delivery systems (DDS). However, both CaCO₃ and HAp have individual draw-backs and limitations in applications. It has been reported that drugs and proteins embedded into the materials are usually loosely bound on the surface of the particles (adsorbed); a condition which may lead to poor drug release. The results showed that the composite had good thermal stability and better surface area and pore (volume and size) properties. Studies on the performance of the composites as a drug delivery agent using ibuprofen as a model drug in simulated gastric fluid revealed that the composite promoted the dissolution of ibuprofen outstandingly. Whereas the low pressure loaded composite showed quicker relief potential (92% release) in 30 minutes with control release over desirable time frame (3h, 20 min), the high pressure loaded composite also exhibited quicker relief potential (80% release) in 30 minutes but with control release over remarkable time frame (6h, 40 min). The implication is that if a patient is administered with ibuprofen loaded into the synthesized composite at low pressure (10.0 MPa), the patient will experience quicker relief (92% release of ibuprofen) in 30 min and which will be sustained for almost 3.5 hours. Similarly, the high pressure (17.0 MPa) loaded ibuprofen will also provide a patient with quicker relief (80% release of ibuprofen) however, the relief in this case will be sustained for longer period; about 6.5 hours. Therefore, the high pressure loaded composite had tremendous effect on the control release of ibuprofen and can be used as effective drug delivery system (DDS) for drugs with similar characteristics.

INTRODUCTION

The anhydrous crystalline polymorph phases of calcium carbonate (CaCO₃): vaterite, calcite and aragonite have received tremendous attention in the literature compared to their hydrated counterparts: monohydrocalcite and hexahydrocalcite (Domingo et al., 2006; Gomez-Villalba et al., 2012). CaCO₃ is used for numerous chemical and industrial applications, and by living organisms (Domingo et al., 2006). Demand for CaCO₃ will therefore continue to increase globally (Montes-Hernandez et al., 2010). Key factors driving this huge demand are the growing applications of nanometric CaCO₃ in the fields of engineering, pharmaceuticals, medicine, as well as in health care, cosmetics and personal hygiene products (Harja et al., 2012). Industrially, CaCO₃ is usually produced by the solid-solid-gas or solid-liquid-gas carbonation routes using Ca(OH)₂ (Gomez-Villalba et al., 2012).

Similarly, hydroxylapatite (HAp) has attracted much attention as the most suitable biocompatible candidate for use especially, in medical applications, coatings and prosthesis. It does not cause pyrogenic and inflammatory reactions; it is nontoxic, and does not form stringy tissues (Hui et al., 2010) when applied in tissue engineering. It has also been utilized in the ceramics and bioceramics industry, pharmaceuticals and as sorbents in environmental pollution control (Eduardo et al., 2012). For wider applications, control of its surface and pore

properties, purity and morphology is most vital and many techniques have been explored to synthesize HAP with improved properties (Kim & Kumta, 2004; Sopyan, 2004).

Meanwhile, substantial research has also been advanced towards the development of inorganic nanocrystals due to the potential applications. One of such important inorganic materials especially suited for application in the medical, pharmaceutical, drug delivery, tissue engineering, bone reconstruction and dental fields is calcium carbonate-hydroxylapatite (CC-HAp) composite (Goldberg et al., 2010). Separately, calcium carbonate and hydroxylapatite are perhaps, the most important and have been used extensively in pharmaceutical and drug delivery systems (DDS). For instance, CaCO₃ has been employed for the imbedding and absorption of functional molecules and drugs (Marloes et al., 2010). Similarly, HAp has been used to encapsulate plasmid DNA, PEG and other drugs (Guoa et al., 2012). However, both CaCO₃ and HAp have individual draw-backs and limitations in applications. It has been reported that drugs and proteins embedded into the materials are usually loosely bound on the surface of the particles (adsorbed); a condition which may lead to poor drug release (Ueno et al., 2005). As a result, several procedures aimed at effectively embedding drugs into inorganic solid matrices have been proposed (Ueno et al., 2005). Combining these versatile materials may alleviate

¹ Department of Mechanical Engineering, Faculty of Engineering, Tamale Technical University, Tamale, Ghana

² Graduate School, Tamale Technical University, Tamale, Ghana.

* Corresponding author: iabdulrauf@tatu.edu.gh

some of their individual draw-backs and lead to wider applications (Goldberg et al., 2010). The combination of porous carbonate hydroxyapatite (CHAp) and tri-calcium phosphate (TCP) has been applied for sustained release of anticancer drugs and antibiotics (Goh et al., 2013). A calcium phosphate (CaP)/ glycerylphosphorylcholine (GPC) and PEG (CaP/GPC-PEG) hybrid porous nanospheres were also used as drug carriers to alleviate multidrug resistance (MDR) (Sun et al., 2012).

Liquids which have their volumes expanded as a result of been pressurized with a gas which has the ability to condense have equally received attention from the research world (Akiem & Poliakoff, 2009). These systems, known as gas expanded liquids (GXLs) comprise of solvents or mixture of solvents which have been used in variety of engineering processes due to their pressure-tunable properties (Akiem & Poliakoff, 2009). Carbon dioxide expanded liquids (CXLs) are the most popularly utilized group among the GXLs due to its obvious advantages (Aaron et al., 2009).

We applied the CO₂-expanded carbonation (CXC) technique for direct and template-free synthesis of high surface area and pore volume CaCO₃-HAp nanoparticle composite with superstructures (Ibrahim et al., 2014a) and investigated the performance of the composites as drug delivery agent using ibuprofen as a model drug in simulated gastric fluid.

Experimental

Materials

Analytical reagent grade Ca(OH)₂ with 95.0% containing ~3% CaCO₃ (Figure 1a) with 61 nm mean crystallite size (as measured by Jade), Phosphoric acid (95.0%) and ethanol (≥ 95.0%) were purchased from Sinopharm Reagent Co. Ltd, China and used as received whereas CO₂ (99.99%) gas was purchased from Linde Gas, Xiamen Corporation Ltd (China). For comparison, CaCO₃ (100%) (Ibrahim et al., 2013) and HAp (100%) (Ibrahim et al., 2015) were produced using previously reported techniques.

Procedure

Illustration of the experimental setup and the reaction procedure are shown in a previous publication (Ibrahim et al., 2013). Briefly, appropriate masses of Ca(OH)₂ and phosphoric acid consisting of Ca/P molar ratio of 2 were measured. The Ca(OH)₂ was transferred to the reaction vessel and the phosphoric acid was gently added to the vessel. To this mixture, 50mL of 4:1 ethanol–water ratio solution was added. The reaction vessel was sealed and heated to 60°C with a water bath (DF-101T, Yuhua-China) under agitation (30 rpm). After thermal equilibrium, CO₂ at 8.0MPa was fed faster (within 30s) into the reactor under continuous agitation to produce a CO₂-expanded suspension for the onward reaction within set time. Products were recovered, washed severally with ethanol to remove traces of water and vacuum dried at 60°C for 12h. Note that each batch experiment was repeated at least three times for reproducibility (Ibrahim et al., 2013; Ibrahim et al., 2014b).

Characterizations

Phase purity and composition of the products were characterized by X-ray diffraction (XRD); data were taken in 2θ° using a step size of 0.02° in 2θs counting range between 5–60° with Cu Kα radiation (Rigaku Ultima IV). The morphology and structure of the particles produced were studied by scanning electron microscopy (SEM; Hitachi, S-4800). Functional group analysis was by Fourier transform infrared spectroscopy (FT-IR; Nicolet 330) within 400–4000 cm⁻¹ using KBr with 4 cm⁻¹ resolution whereas the surface area and pore properties of the powders were studied by Brunauer Emmett and Teller (BET; Micromeritics ASAP 2020, USA) analysis. The XRD patterns for commercial Ca(OH)₂, CaCO₃,

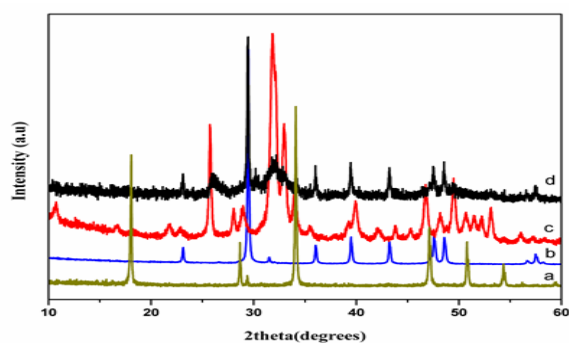


Figure 1. XRD patterns for a): Ca(OH)₂, b): Calcite, c): HAp and d): typical Calcite-HAp composite

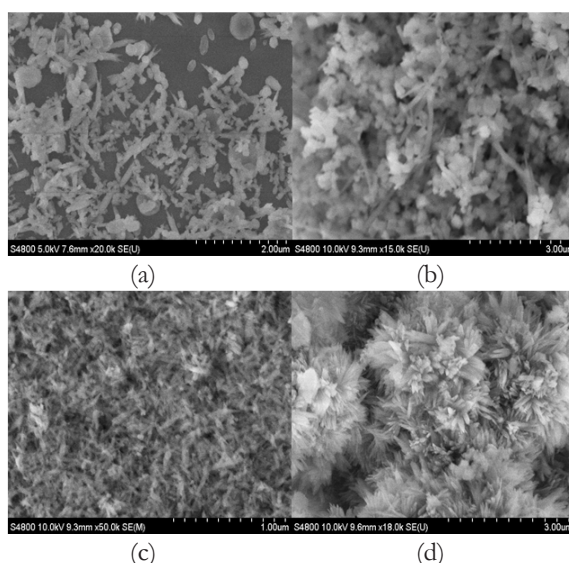


Figure 2. SEM images for a): Ca(OH)₂, b): Calcite from CO₂-expanded carbonation, c): HAp produced and d): typical synthesized Calcite-HAp composite.

HAp and typical composite product are shown in Figure 1. The main characteristic peaks for Ca(OH)₂ in 2θ are 18.1°, 28.7°, 34.1°, 47.1°, 50.7° and 54.4° (Figure 1a). Those for CaCO₃ are 29.4°, 36.0°, 39.4°, 43.1°, 47.5° and 48.5° (Figure 1b) whereas those for HAp are 25.9°, 31.7°, 32.2°, 32.9°, 46.7° and 49.4° (Figure 1c). The typical composite product had characteristic peaks at 25.9°, 31.7°, 29.4°, 36.0°, 39.4°, 43.1°, 47.5° and 48.5° (Figure 1d). No characteristic peaks for Ca(OH)₂ were observed in the composite product indicating complete conversion

of the reactant (Figure 1 a; d). This is a confirmation of the synthesis of CaCO₃-HAP composite because the composite exhibited the characteristic peaks for both CaCO₃ and HAP (Figure 1 b; d).

RESULTS AND DISCUSSIONS

Effect of temperature

XRD patterns for the effect of temperature are shown in Figure 3. The reaction temperatures above the critical temperature of CO₂ ($T \geq 35^\circ\text{C}$) yielded complete conversions to pure CaCO₃-HAP composites. The

products of these reactions exhibited similarity in the XRD patterns (Figure 3a-d). However, the reaction temperatures below the critical temperature of CO₂ led to emergence of new calcium phosphate compound: brushite (CaHPO₄·(H₂O)₂) with diffraction peaks at $2\theta = 11.7^\circ, 18.0^\circ$ and 20.9° (Figure 3, dotted inset).

The XRD analysis revealed that the calcite content decreased with decreasing temperature from 60°C to 40°C whereas HAp content increased correspondingly with these temperatures. However, the calcite content increased with further decreasing temperature from 35°C

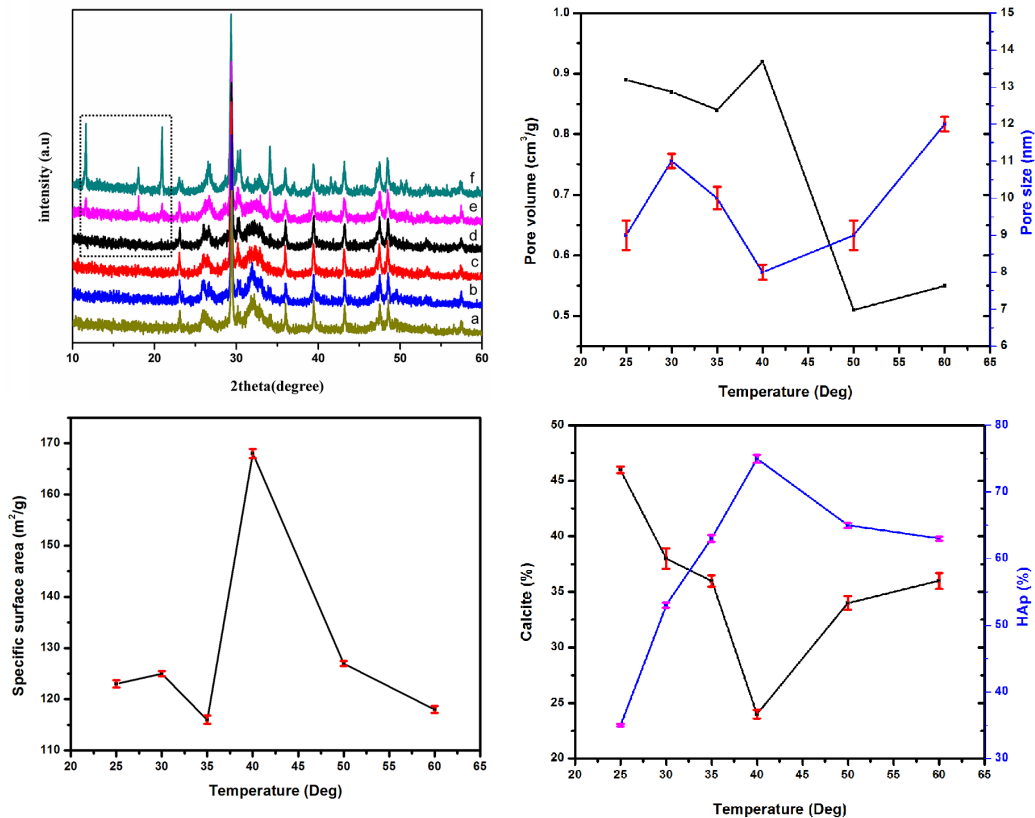


Figure 3. Influence of temperature on calcite and HAp XRD patterns (inset shows brushite peaks), pore properties, surface area and calcite and HAp content (%) at 8MPa in 30min

to 25°C with corresponding decrease in HAp content. Even so, the 30°C and 25°C samples contained brushite (Figure 3; Table S1). Therefore, the highest calcite content was realized at the lowest temperature condition (25°C) whereas the highest HAp content was at the moderate temperature condition (40°C).

The BET analyses of the composites are also shown in Table S1. The specific surface area exhibited a contrary trend to the content of calcite. It increased with decreasing temperature from 60°C to 40°C. However, it continues to decrease at 30°C but increased at 30°C and then decreased again albeit slightly at 25°C (Table S1). Therefore, the surface area was dependent on the content of calcite and HAp or both. Specifically, the surface area was directly proportional to the content of HAp and inversely proportional to the calcite content (Table S1) from 60°C to 35°C.

The SEM images of the products from the temperature conditions (60°C, 50°C, 40°C, 30°C) are shown in Figure 4.

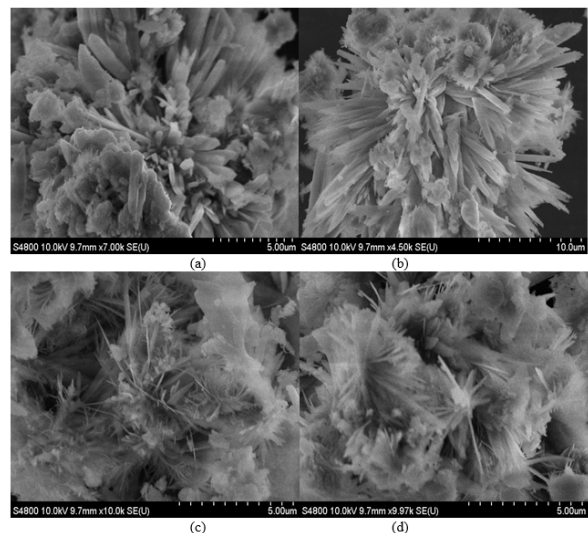


Figure 4. SEM images for effect of reaction temperature at a): 60°C, b): 50°C, c): 40°C, d): 30°C at 8MPa in 30min

Besides the particle sizes, the structure and morphology of the particles were almost the same; mixture of rod-like, plate-like and flower-like structures. However, the

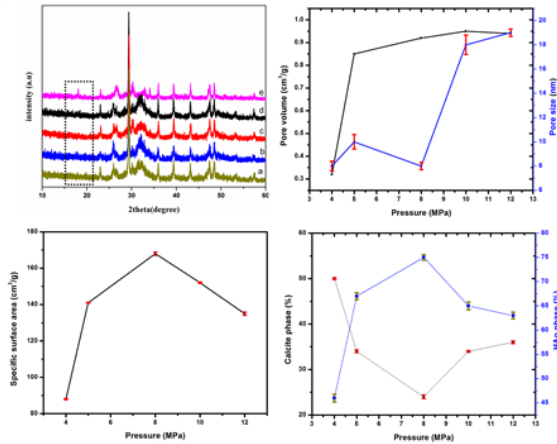


Figure 5. Influence of pressure on calcite and HAP XRD patterns (inset shows monetite peaks), pore properties, surface area and calcite and HAP content (%) at 40°C, 30min

size of the rod-like particles for the 40°C and 30°C were smaller compared to those obtained from the 60°C and 50°C, perhaps, confirming their better surface properties (Table S1).

Effect of pressure

XRD patterns for effect of different pressures are shown in Figure 5. Almost all the pressures (5MPa, 8MPa, 10MPa and 12MPa) gave complete conversions (pure CaCO₃-HAP composites) except for 4MPa. There was about 3±0.2% (Table S2) monetite (PDF2: 01-071-1759) in the apatite phase at about 2θ = 18.1° (Figure 5; dotted inset in XRD pattern) at this pressure.

All the characteristic peaks for the respective phases

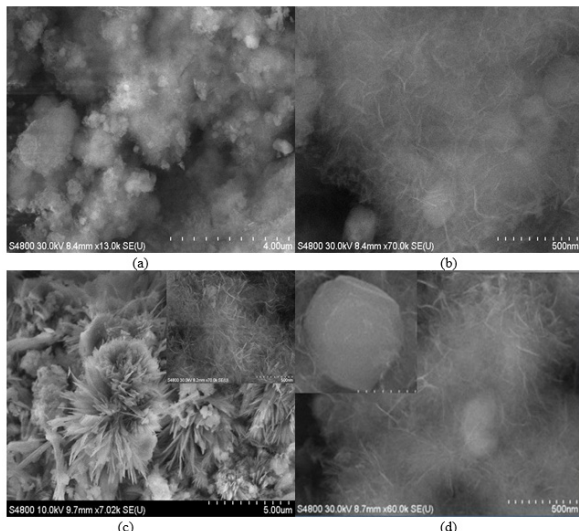


Figure 6. SEM images of composite nanoparticles obtained at different pressures: (a) 4.0MPa, (b) 5.0MPa, (c) 8.0MPa, and (d) 12.0MPa, at 40°C, 30min (calcite, HAP, monetite) were observed (XRD patterns in Figure 5). Rietveld analysis of the XRD patterns showed that the calcite content decreased at 4MPa to 8MPa but increased at 12MPa. However, the HAP phase increased

4MPa to 8MPa but decreased finally at 12MPa (Table S2). The BET specific surface and pore property analyses of the composites are also shown in Table S2. The surface

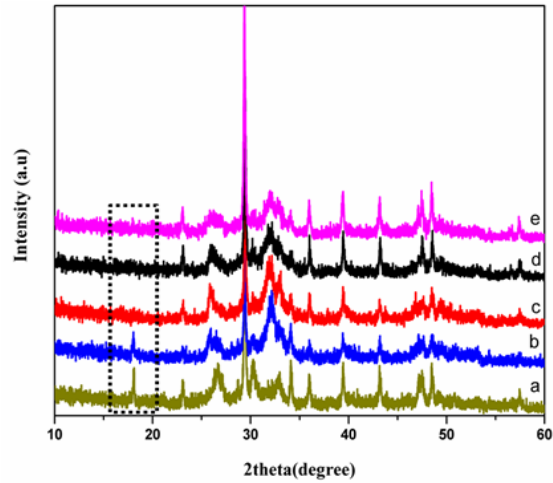


Figure 7. XRD patterns for influence of reaction time at a): 5min, b): 10min, c): 15min, d): 30min and e): 60min (inset is peaks indicating presence of brushite and monetite) at 40°C and 4MPa

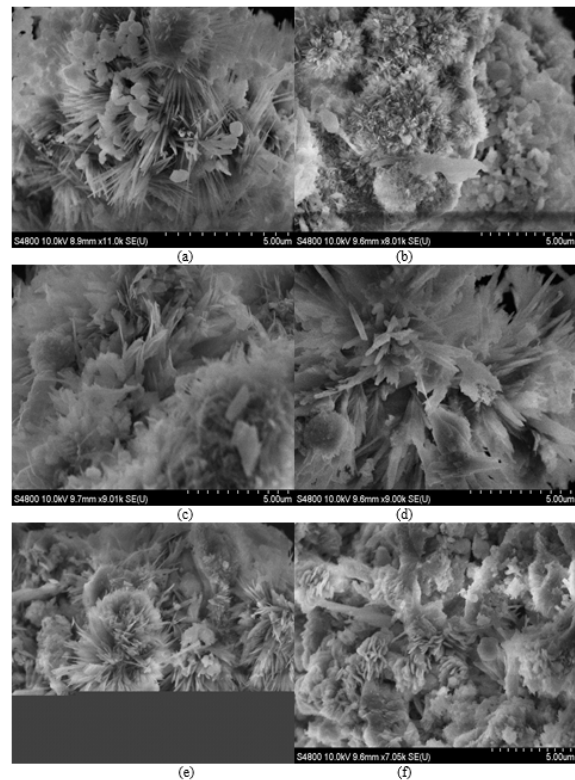


Figure 8: SEM images for effect of reaction time at a): 0 min, b): 5min, c): 10min, d): 15min, e): 30min and f): 60min at 40°C and 4MPa

area was inversely proportional to the calcite content at 4MPa to 8MPa but directly proportional to the HAP content at 8MPa to 12MPa. The surface area increased with decrease in the calcite phase but increase in the HAP content at 4MPa to 8MPa. However, the surface area decreased with increase in the calcite phase but decrease in the HAP content at 8MPa to 12MPa.

Effect of time

XRD patterns for effect of different times are shown in Figure 7. All the times gave complete conversions of the starting material; Ca(OH)₂ (Table S3) but not all the conditions yielded pure CaCO₃-HAP composites. All the Ca(OH)₂ was not transformed to the desired composite. There was brushite and monetite in <1 minute, monetite in 5 min and monetite in 10 min (Table S3). The SEM images for the products at the various times are shown in Figure 8. The structure and morphology of the particles appear to the same consisting of mixture of agglomerated spherical, rod-like, plate-like and flower-like structures.

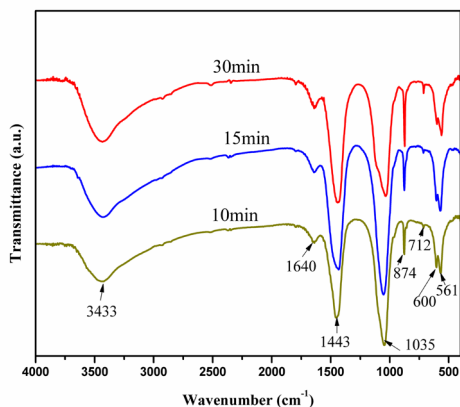


Figure 9. IR spectra of the CaCO₃-HAP composites at different reaction times

Functional group analysis

Functional group analysis was also conducted on the CaCO₃-HAP composite using FTIR between 400cm⁻¹ to 4000cm⁻¹ (Figure 9). All the functional groups (OH-, H₂O, PO₄³⁻ and CO₃²⁻) belonging to the composite were present and appeared at the usual wave lengths. Water (H₂O) appeared at about 3433 cm⁻¹ and 1640 cm⁻¹

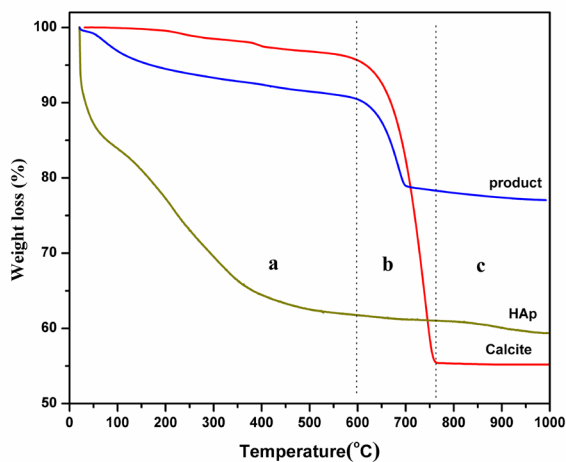


Figure 10. Thermogravimetric analysis of the composite, pure HAp and pure calcite

1; PO₄³⁻ bending mode at about 565, 603, 874, 1039cm⁻¹; OH- stretching at about 3745 cm⁻¹ and CO₃²⁻ at about 874 and 1422cm⁻¹. In fact, calcite has characteristic bands at 874 cm⁻¹ and 712 cm⁻¹. Radical CO₃²⁻ for carbonated hydroxyapatite (CHAp) has absorption peak

at 1443 cm⁻¹ (Lafon et al., 2008) which was absent in the composite sample (Figure 9). In fact, XRD analysis had shown that CaCO₃-HAP Composite was produced which is consistent with the results from the FTIR analysis.

Thermal stability analysis

Thermal stability analysis was conducted using SDT-Q600 analyzer in N₂ atmosphere from room temperature (RT) to 1000°C at a heating rate of 10°C/min and the results are shown in Figure 10.

The total weight loss of the composite sample over the entire heating period (at RT to 1000°C) was about 20%, indicating good thermal stability.

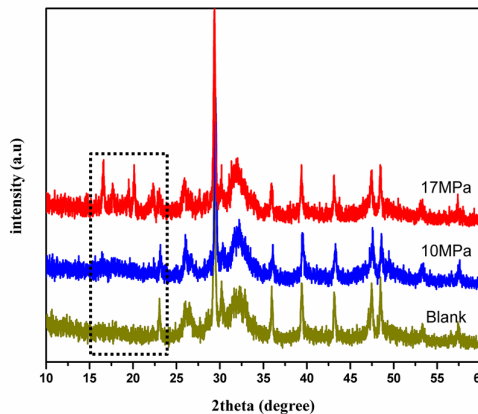


Figure 11. The XRD patterns for products before and after supercritical loading at low and high pressures; inset: ibuprofen loaded.

Drug loading and dissolution

Solute-saturated supercritical loading procedure (Song et al, 2017; Ibrahim et al., 2019) was used to load ibuprofen into the composite sample produced at 40°C and 8MPa in 30min. The composite contained 36.4% CaCO₃ and 63.6% HAP with 133.60 m²/g specific surface area, 0.74 cm³/g pore volume and 10.60 nm pore diameter.

XRD patterns of the samples before and after the supercritical loading experiments are shown in Figure 11 (inset is diffraction peaks for ibuprofen demonstrating

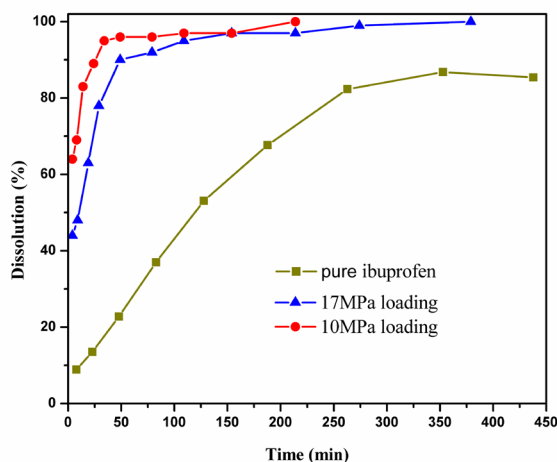


Figure 12. Dissolution profiles of composite loaded with Ibuprofen in hydrochloric acid-potassium chloride buffer solution

effective loading at $2\theta = 16.6^\circ$, 17.7° and 20.2°). The diffraction peaks for ibuprofen was not clearly visible at lower pressure (10.0 MPa) loading perhaps, due to the minimal amount of loading (0.17g ibuprofen/g composite). At higher pressure (17.0MPa) loading, the diffraction peaks for ibuprofen was clearly visible attributed to substantial amount of ibuprofen loaded (0.28g ibuprofen/g composite) and/or deposited on the surface of the composite (Chen et al., 2013; Ibrahim et al., 2015).

After the supercritical loading, 2.3 mg of the ibuprofen-composite samples loaded at 10.0 MPa and 17.0 MPa were dissolved in simulated gastric fluid (HCl-KCl buffer solution, $\text{pH} = 1.4 \pm 0.02$) with a test apparatus (RCA-1A, Huanghai Medicine & Drug Testing Instruments co., Ltd., Shanghai, China) at $37 \pm 0.5^\circ\text{C}$ with a paddle speed of 100 ± 1 rpm (Chen et al., 2013) for the dissolution test and the results are shown in Figure 12.

The low pressure (10.0 MPa) loaded composite released 92% of the loaded ibuprofen within 30 min whereas the high pressure (17.0 MPa) loaded composite released 80% of the loaded ibuprofen within the same time period. However, the dissolution of pure ibuprofen sample was much lower; 18% of the loaded ibuprofen was released within 30 min. The high release of the loaded ibuprofen from the composites is due to the fact that the loaded ibuprofen particles were dispersed in the interior and the surface of the composite. This increased the contact surface with the buffer, thereby improving the dissolution rate.

The low pressure (10.0 MPa) loaded composite gave faster dissolution compared to the high pressure (17.0 MPa) loaded composite up until about 150 min because of the less loading effect. Majority of the ibuprofen was dispersed and deposited uniformly on the surface of the low pressure composite leading to faster dissolution rate. Another important observation is that the low pressure loaded composite exhibited quick and faster release of the drug; all the ibuprofen was released within 200 min whereas the high pressure loaded composite exhibited slow and controlled release of the drug over 400 min.

The implication of the results of the study is that if a patient was administered with a drug (for instance, ibuprofen) loaded into the synthesized composite ($\text{CaCO}_3\text{-HAp}$) at low pressure (10.0 MPa), the patient will experience quicker relief (92% release of ibuprofen) in 30 min which will be sustained for almost 3.5 hours. The high pressure (17.0 MPa) loaded drug will also provide the patient with quicker relief (80% release of ibuprofen) however, the relief in this case will be sustained for longer period; about 6.5 hours.

Therefore, the high pressure loaded composite had tremendous effect on the controlled release of ibuprofen and can be used as effective drug delivery system (DDS) for drugs with similar characteristics.

CONCLUSIONS

We employed Gas expanded liquids (GXLs) technology to

synthesize calcium carbonate-hydroxylapatite composite nanoparticles and investigated the effects of reaction parameters on the properties of the composites. Based on the results we conclude that the composite had good thermal stability, better surface area and pore properties. The performance of the composites as a drug delivery agent using ibuprofen as a model drug in simulated gastric fluid was commendable. Whereas the low pressure loaded composite showed quicker relief potential (92% release) in 30 minutes with controlled release over desirable time frame (3h, 20 min), the high pressure loaded composite also exhibited quicker relief potential (80% release) in 30 minutes with controlled release over remarkably longer time frame (6h, 40 min).

Therefore, the loaded composites had tremendous effect on the controlled release of ibuprofen and can be used as effective drug delivery system (DDS) for drugs with similar characteristics globally.

Acknowledgments

This work is supported by the Ghana government book and research allowance.

Conflict of interest

The authors declare no conflict of interests

REFERENCES

- Aaron, M. S., Hutchenson, K., & Subramaniam, B. (2009). *Gas-Expanded Liquids: Fundamentals and applications*, in: Gas-Expanded Liquids and Near-Critical Media, American Chemical Society, Washington, DC, 3-37.
- Akien, G. R., & Poliakoff, M. (2009). A Critical Look at Reactions in Class I and II Gas-Expanded Liquids Using CO_2 and other Gases. *Green Chemistry*, 11, 1083-1100.
- Chen, W. W., Hu, X. H., Hong, Y. Z., Su, Y. Z., Wang, H. T., & Li, J. (2013). Ibuprofen Nanoparticles Prepared by a PGSS™-Based Method. *Powder Technology* 45, 241–250.
- Domingo, C., Loste, E., Gomez-Morales, J., Garcia-Carmona, J., & Fraile, J. (2006). Calcite Precipitation by a High-Pressure CO_2 Carbonation Route. *Journal of Supercritical Fluids*, 36, 202-215
- Eduardo da Silva, A. B., Costa, C. A. E., Vilar, V. J. P., Botelho, C. M. S., Larosi, M. B., Saracho, J. M. P., & Boaventura, R. A. R. (2012). Water Remediation Using Calcium Phosphate Derived from Marine Residues. *Water, air, and soil pollution*, 223, 989-1003
- Goh, Y.-F., Shakir, I., & Hussain, R. (2013). Electrospun fibers for Tissue Engineering, Drug Delivery, and Wound Dressing. *Journal of Material Science*, 48, 3027–3054
- Goldberg, M. A., Smirnov, V. V., Kutsev, S. V., Shibaev, T. V., Shvornev, L. I., Sergeev, N. S., Sviridov, I. K., & Barinov, S. M. (2010). Hydroxyapatite–Calcium Carbonate Ceramic Composite Materials. *Inorganic Materials*, 46, 1269–1273
- Gomez-Villalba, L. S., Lopez-Arce, P., Alvarez de Buergo, M., & Fort, R. (2012). Atomic Defects and their Relationship to Aragonite-Calcite Transformation in

- Portlandite Nanocrystal Carbonation. *Crystal Growth & Design*, 12, 4844-4852
- Guoa, Y.-P., Yao, Y.-B., Guo, Y.-J., & Ning, C.-Q. (2012). Hydrothermal Fabrication of Mesoporous Carbonated Hydroxyapatite Microspheres for a Drug Delivery System, *Microporous and Mesoporous Materials* 155, 245–251
- Harja, M., Cimpeanu, C., & Bucur, R. D. (2012). The Influence of Hydrodynamic Conditions on The Synthesis of Ultra-Thin Calcium Carbonate, *Journal of Food, Agriculture & Environment*, 10, 1191-1195
- Hui, P., Meena, S. L., Singh, G., Agarawal, R. D., & Prakash S. (2010). Synthesis of Hydroxyapatite Bio-Ceramic Powder by Hydrothermal Method. *Journal of Minerals and Materials Characterization Engineering* 9, 683-692
- Ibrahim, A-R., Benoit, R., Suo, X., Li, X. Y., Huang, Y., Ma, G. F., & Li, J. (2019). Ultra-Fast Route to Synthesizing Biogenic Carbonate Hydroxyapatite: Consequence of a High-Pressure Solid-Solid Preparation Technique. *Chemical Engineering & Processing: Process Intensification*, 142, 107549
- Ibrahim, A-R., Gong, Y., Hu, X. H., Hong, Y. Z., Su, Y. H., Wang, H. T., & Li, J. (2013). Solid-gas Carbonation Coupled with Solid Ionic Liquid for Synthesis of CaCO₃. Performance, Polymorphic Control and Self-catalytic Kinetics. *Industrial and Engineering Chemistry Research*, 52, 9515–9524
- Ibrahim, A-R., Zhang, X. L., Hong, Y. Z., Su, Y. H., Wang, H. T., & Li, J. (2014b) Instantaneous Solid-Liquid-Gas Carbonation of Ca(OH)₂ and Chameleonic Phase Transformation in CO₂ Expanded Solution. *Crystal Growth & Design*, 14, 2733–2741
- Ibrahim, A-R., Zhou, Y., Li, X. Y., Chen, L., Hong, Y. Z., Su, Y. Z., Wang, H. T., & Li, J. (2015). Synthesis of rod-like hydroxyapatite with high surface area and pore volume from eggshells for effective adsorption of aqueous Pb (II). *Materials Research Bulletin*, 62, 132–141
- Ibrahim, A-R., Zhu, L. H., Xu, J., Hong, Y. Z., Su, Y. H., Wang, H. T., Chen, B. H., & Li, J. (2014a). Synthesis of Mesoporous Alumina with CO₂-Expanded Carbonation and its Catalytic Oxidation of Cyclohexanone. *Journal of Supercritical Fluids*, 92, 190-196
- Kim, I.-S., & Kumta, P.N. (2004). Sol-gel Synthesis and Characterization of Nanostructured Hydroxyapatite Powder. *Material Science and Engineering B*, 111, 232-236
- Marloes. M. J. K., Angus P. R. J., Georgina K. S., Henk H. D., Richard A. E., Andrew M. S., Edouard C. N., Joan K. H., & Frank C., (2010). Targeting of cancer cells using click-functionalized polymer capsules, *Journal of the American Chemical Society*, 132, (45), 15881–15883
- Montes-Hernandez, G., Daval, D., Chiriac, R., & Renard, F. (2010). Growth of Nanosized Calcite through Gas-Solid Carbonation of Nanosized Portlandite under Isobaric Conditions. *Crystal Growth & Design* 10, 4823-4830
- Song, L., Chen, Y., Chen, K., Hu, X. H., & Li, J. (2017). Solute-Saturated Supercritical CO₂ Loading of 2-Phenylethyl Alcohol in Silica and Activated Carbon: Measurement and Mechanism. *The Journal of Supercritical Fluids* 128, 378-385
- Sopyan, I. (2004). Proceedings of the 3rd Annual Conference of the Asia Pacific Nanotechnology Forum. *Shanghai, China*, 180–188
- Sun, Y., Chen, X.-Y., Zhu, Y.-J., Liu, P.-F., Zhu, M.-J., & Duan, Y.-R. (2012). Synthesis of Calcium Phosphate/GPC-mPEG Hybrid Porous Nanospheres for Drug Delivery to Overcome Multidrug Resistance in Human Breast Cancer. *Journal of Materials Chemistry*, 22, 5128-5136
- Ueno, Y., Futagawa, H., Takagi, Y., Ueno, A., & Mizushima, Y. (2005). Drug Incorporating Calcium Carbonate Nanoparticles for a New Delivery System, *Journal of Controlled Release*, 103, 93-98